Robotica (1999) volume 17, pp. 601–612. Printed in the United Kingdom © 1999 Cambridge University Press

Experimental comparison of decentralized controllers for industrial robots*

Antonio Visioli† and Giovanni Legnani††

(Received in Final Form: June 19, 1999)

SUMMARY

In this paper we present an experimental comparison between different decentralized controllers for industrial robot manipulators. In spite of the fact that robot manipulators are highly nonlinear and coupled multivariable systems, decentralized controllers have been widely adopted in industrial environments for trajectory tracking, because of their simplicity and their fault tolerance feature. Different kinds of controllers have been investigated: the typical PID-based controller, a nonlinear three-term controller devised by Tarokh, and a variable structure control law, a discontinuous integral control, both in the continuous and in the discretised version. Allowances are made for the tuning of the parameters in order to obtain low tracking errors. Results show that better performances are obtained by controllers other than PID, especially by the discontinuous integral control, so that they appear to be particularly appropriate for the use in industrial robots.

KEYWORDS: Robot manipulators; Robot control; Decentralized control; PID control; Variable structure control.

1. INTRODUCTION

Dexterous and skilled motions in industrial robot manipulators require reliable and robust joint controllers in order to guarantee low trajectory tracking errors, despite uncertainties in the robot dynamics and external disturbances. It is well-known that a mechanical manipulator is a highly coupled nonlinear system whose parameters are very difficult to estimate, so that the control design is a very hard task which has been addressed by a large number of researchers. Many proposed control schemes take into account the full robot dynamics with the aim of cancelling the nonlinearities and decoupling the system. Then, a linear control law is applied.[1] Adaptive control can be exploited in this context in order to cope with system uncertainties.[2] However, this results in a significant increasing of the control architecture complexity so that these schemes are very difficult to implement in practice in an industrial setting. For these reasons, decentralized control, in which each joint is controlled separately by a simple position servoloop, has been widely adopted by the robotics industry. This is mainly due to the ease of implementation and because of the fault tolerance feature since only one joint is affected in the case of a component failure. This allows the robot to continue operating, although in a limited capacity, so that it can be placed in a safe position by means of other unaffected joints. It is apparent how this characteristic is particularly desirable in applications such as hazardous material handling. Furthermore, fault detection and isolation is faster and more convenient with independent joint control. Several decentralized adaptive control schemes have been presented in the literature (see e.g. references 3–7). However, the most adopted controller for industrial robots are still based on Proportional-Integral-Derivative (PID) controllers, with the addition of functionalities (filters, feedforward actions and so on) that can be exploited to improve the performances. This seems to be due to the fact that PID controllers have a simple structure, are widely known, easy to tune and provide adequate performances for basic pick-and-place tasks, where only point-to-point motion is of concern. Moreover, despite the publication of many theoretical works, not many experimental results have been discussed in the literature,[8–10] and a full comparison between PID and novel techniques has not been deeply performed. In order to replace conventional controllers in the industrial context, it is necessary to show that it is possible to overcome the limits of PID controllers in trajectory tracking; besides, a full understanding of the significance of all the parameters of the new control laws and a detailed discussion of the problems that might arise still have to be provided.

The aim of this paper is to analyse and compare different decentralized controllers in order to provide information on their use and the results they can achieve. Among the several control laws provided in the literature, we selected a few of them whose theoretical analysis has been performed in details and that are easy to implement and therefore suitable for industrial applications; they do not require any knowledge of the robot dynamics and the stability proof is obtained under mild conditions. These controllers are the PID-based ones where the control scheme basically consists of an inner velocity loop and an outer position loop, a nonlinear three term controller proposed by Tarokh[11] and the discontinuous integral control (both in the continuous and discretised version), which is a kind of variable structure sliding mode controller, which has been recently devised.[12–16]

The paper is organized as follows: In Section 2 the adopted controllers are described. In Section 3 the experimental setup is presented. Experimental results are shown in

* This work was partially supported by MURST.

† Dipartimento di Elettronica per l'Automazione, University of Brescia, Via Branze, 38–25123 Brescia (Italy).
e-mail: visioli@bsing.ing.unibs.it
†† Dipartimento di Ingegneria Meccanica, University of Brescia (Italy). e-mail: legnani@bsing.ing.unibs.it

https://doi.org/10.1017/S0263574799001897 Published online by Cambridge University Press

Section 4 and discussed. The effect of friction compensation is examined in Section 5. Conclusions are drawn in the last section.

2. DECENTRALIZED CONTROLLERS FOR MECHANICAL MANIPULATORS

It is well-known that the dynamic model of a n-joint manipulator can be written as follows:

$$M(\theta)\ddot{\theta}+C(\theta,\dot{\theta})\dot{\theta}+g(\theta)+f(\dot{\theta})+u_d(t)=u(t)$$

where θ is the $n\times 1$ joint angle vector, $u(t)$ is the $n\times 1$ input torque vector, $M(\theta)$ is the $n\times n$ inertia matrix, $C(\theta,\dot{\theta})$ is the $n\times n$ matrix representing the centrifugal and Coriolis terms, $f(\dot{\theta})$ is the $n\times 1$ vector of the frictional terms, $g(\theta)$ is the $n\times 1$ vector of the gravity terms, and $u_d(t)$ is a $n\times 1$ vector representing unknown disturbances. Figure 1 shows a typical scheme of a decentralized or independent joint control, where the torque u_i to be generated by the i-th actuator is based only on the value of the position of the i-th joint and on its time derivatives:

$$u_i=u_i(\theta_i,\ \dot{\theta}_i,\ \theta_{di},\ \dot{\theta}_{di}) \quad i=1,\ldots,n.$$

Generally, defining the position error as $e_i(t)=\theta_{di}-\theta_i$, equation (1) is rewritten as:

$$u_i=u_i(e_i,\dot{e}_i) \quad i=1,\ldots,n.$$

In this framework, we chose different decentralized control laws that seem particularly suitable to be employed in an industrial context, due to their simplicity.

2.1 PID control

The typical PID-based control for robot manipulators basically consists of two nested regulators, i.e. an inner loop for velocity and an outer loop for position regulation, as shown in Figure 2. It has to be noted that the velocity control loop cannot be necessary (which means that the motor amplifiers are configured in "current" mode), but when it is present, it is generally tuned first and is often implemented by an analog device embedded in the drive of the motor. On the contrary, the position control loop is always realized by a digital microprocessor. In this paper we adopted the two loops scheme, since we have seen it provides the best results for our testbed. Both the two loops have been implemented in software.

The well-known general expression of a PID controller is the following:

$$u(t)=K_p\left(e(t)+\frac{1}{T_i}\int_0^t e(\tau)d\tau+T_d\frac{de(t)}{dt}\right), \qquad (2)$$

where K_p is the proportional gain and T_i and T_d are, respectively, the integral and derivative time constants. In addition to the classical three actions, different functionalities can be selected by the user to improve the tracking performances. Specifically, the input of the PD part can be low-pass filtered to avoid the amplification of high-frequency noise and the value of the integral term can be limited, as well as the maximum error to be integrated, to avoid the wind-up effect. Moreover, feedforward terms (i.e. the commanded velocities and accelerations are multiplied by scalar factors to provide an additional control action) can be utilized to increase the transient performances. The resulting control variable has to be saturated to avoid that the maximum DAC output is exceeded and, most important, that velocity/torque limits of the motors are not surpassed and it can be also low-pass filtered to prevent the excitation of high-frequency modes and the occurring of vibrations. It is worth stressing that the properties of the Proportional-Integral-Derivative terms are generally well understood by the industrial operators and many tuning techniques have been devised.[17] The tuning of the other additional parameters is more critical and it might not be worthy to use them. For our system, we found that only low-pass filtering the error derivative signal was useful to improve the performances for all the experimented trajectories.

2.2 Tarokh's nonlinear three-term control

The nonlinear control law proposed by Tarokh in 1996,[11] consists of three terms and is described by the following expression:

$$u_i(t)=k_i\eta_i(t)+p_i\eta_i(t)\int_0^t\eta_i^2(\tau)\,d\tau + q_i\,sgn(\eta_i(t))\int_0^t|\eta_i(\tau)|\,d\tau \quad i=1,\ldots,n \qquad (3)$$

where u_i is the torque applied to the motor of the i-joint, k_i, p_i and q_i are constant scalar gains, and $\eta_i(t)$ is defined as

$$\eta_i(t)=\lambda_i e_i(t)+\dot{e}_i(t) \quad i=1,\ldots,n$$

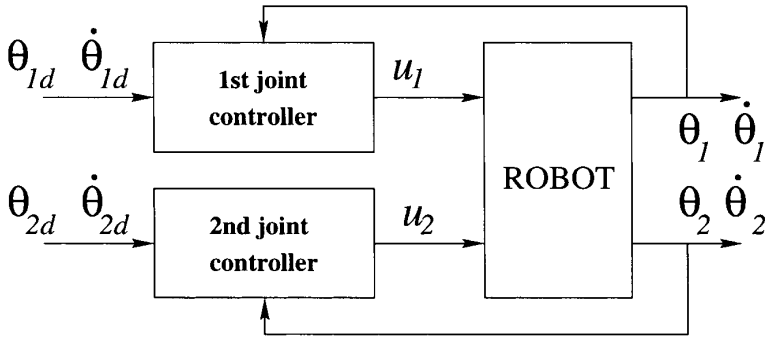

Fig. 1. General scheme of a decentralized 2 d.o.f. robot control.

https://doi.org/10.1017/S0263574799001897 Published online by Cambridge University Press

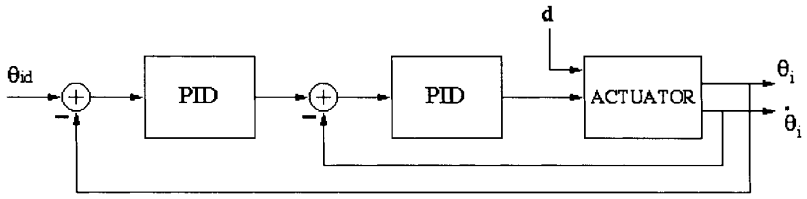

Fig. 2. Control scheme of one robot joint with PID, where d is the disturbance due to the dynamic coupling.

where λ_i is a constant positive scalar. The asymptotic stability of tracking error is demonstrated by using the Lyapunov stability theorem. Moreover, theory and simulation assure that this control system is robust to torque disturbances and to a class of unmodelled dynamics. The last control torque component in (3) contains a signum function that can result in chattering effect. In order to avoid this effect, the signum can be replaced by a saturation function of the form:

$$sat(\eta_i) = \begin{cases} \eta_i/\varepsilon & |\eta_i| < \varepsilon \\ sgn(\eta_i), & otherwise \end{cases}$$

where ε is the boundary layer thickness. The asymptotic stability is preserved.[18] This third term produces a steady-state torque that is needed to hold the arm against gravity, whilst the first two components contribute to the transient response, since it is $\eta_i = 0$ at the steady-state.

Simulation results seems very promising but no experiments have been provided in the literature until now to verify the real effectiveness of the controller.

2.3 Discontinuous integral control

Variable-structure sliding mode control has been widely investigated since the 50s because of its effectiveness in solving the problem of robust stabilization of nonlinear multivariable systems[19] and some versions of it have already been effectively experimented on industrial robots (see e.g. reference 8). An interesting approach, which seems particularly appropriate for application in mechanical systems, is the recently developed discontinuous integral control, both in the continuous and discrete version.[12–16] The aim of this kind of control is to reduce the chattering introduced by the characteristic switching term of the controller, by adding an integrator with a nonlinear switching input whose purpose is to track the unknown disturbances. In this way, the switching term has to compensate only the difference between the real disturbances and its estimations, so that its effect can be significantly reduced. If we choose the following sliding surface:

$$\sigma(t) = ce(t) + \dot{e}(t)$$

where $c > 0$, then, for the continuous-time case, the expression of the torque command can be stated as (i = 1, ..., n):

$$\begin{aligned} u_i(t) &= l_i\sigma(t) + k_i \mathrm{sgn}(\sigma_i(t)) + \tilde{\psi}_i(t) \\ \dot{\tilde{\psi}}_i(t) &= h_i \int_0^t \mathrm{sgn}(\sigma_i(\tau))d\tau \end{aligned} \qquad (4)$$

where l_i, k_i and h_i are constant parameters and $\tilde{\psi}_i(t)$ is an estimation of an external disturbance $\psi_i(t)$ which is assumed to be continuous and to satisfy the following conditions:

$$|\psi_i(t)| < \Delta_0; \quad |\dot{\psi}_i(t)| < \Delta_1.$$

It can be demonstrated that if parameters l_i, k_i and h_i are chosen in such a way that

$$l_i > 0;\ k_i > 0;\ h_i > \Delta_1;\ h_i l_i k_i > \Delta_1^2(1 - \ln 2);$$

then the controlled system is globally stable and after a finite time a sliding mode arises on the surface σ_i, so that the error asymptotically converges to zero. We will refer to the simple discretized version of (4) as DIC. However, this simple discretized version of (4) can be slightly modified in order to try preventing oscillations, once the estimation of the disturbance is constant.[15,16] It follows that the torque command for the discretised discontinuous integral control (DDIC) can be written as:

$$\begin{aligned} u_i(n) &= k_i \mathrm{sgn}(\sigma_i(n)) + \tilde{\psi}_i(n) \\ \tilde{\psi}_i(n) &= \tilde{\psi}_i(n-1) + k_{e_i}\left[\frac{\Delta\sigma_i(n)}{T_s} + k_i \mathrm{sgn}(\sigma_i(n-1))\right] \end{aligned} \qquad (5)$$

where $\Delta\sigma_i(n) = \sigma_i(n) - \sigma_i(n-1)$, T_s is the sampling time, k_e is a new design parameter and

$$\left[\frac{\Delta\sigma_i(n)}{T_s} + k_i \mathrm{sgn}(\sigma_i(n-1))\right] = \gamma_i(n) \qquad (5)$$

can be viewed as a disturbance estimation error.

Denote by $\bar{\psi}_i(n)$ the mean value of the external disturbance in the time interval $[(n-1)T_s, nT_s]$:

$$\bar{\psi}_i(n) = \frac{1}{T_s}\int_{(n-1)Ts}^{nT_s} \psi_i(t)\,dt.$$

If the discrete derivative of the disturbance is bounded, that is

$$\left|\frac{\bar{\psi}_i(n) - \bar{\psi}_i(n-1)}{T_s}\right| < \Delta_\psi$$

then the estimation error $\gamma_i(\infty)$ is also bounded: $\gamma_i(\infty) = \Delta_\psi T_s$. When the sampling time $T_s \to 0$, the estimation error $\gamma(n)$ tends to zero. So, choosing the amplitude of the switching term k_i such that $k_i > \Delta_\psi T_s$ we have $|\gamma_i(n)| < k_i$ so that a discrete sliding mode occurs in the system.

https://doi.org/10.1017/S0263574799001897 Published online by Cambridge University Press

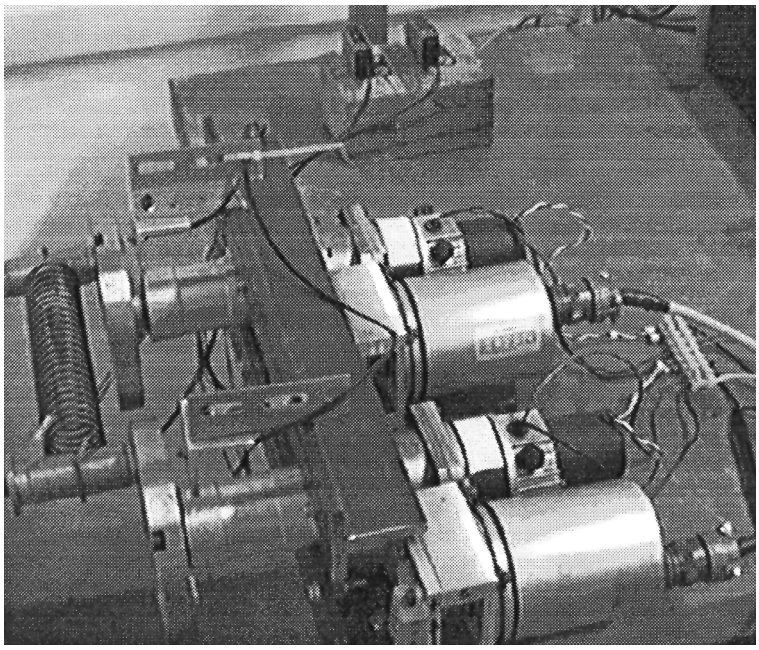

Fig. 3. The experimental setup.

3. EXPERIMENTAL SETUP

Practical experimentations have been performed on a test bed built on purpose and shown in Figure 3. To better reproduce the phenomena usually found in industrial robots, the system has been assembled using components extracted by an actual manipulator. Two DC motors rotate two flywheels by means of two Harmonic Drives (reduction gears) with a reduction ratio of 100. The dynamic coupling between the two d.o.f. has been simulated, adding a spring attached to two pins. The torque generated by the spring depends on the angular positions of the two flywheels and simulates, to a certain extent, the effect of the gravity present in many manipulators. Each motor is equipped with a tachometer and with an incremental encoder to measure, respectively, the angular velocity and rotation. One encoder step corresponds to a rotation of $\pi \cdot 10^{-5}$ rad of the flywheel. The dynamic equation of the system is simply:

$$\begin{bmatrix} J_1 & 0 \\ 0 & J_2 \end{bmatrix} \begin{bmatrix} \ddot{\theta}_1 \\ \ddot{\theta}_2 \end{bmatrix} + \begin{bmatrix} f_1(\theta_1, \theta_2) \\ f_2(\theta_1, \theta_2) \end{bmatrix} + \begin{bmatrix} g(\dot{\theta}_1) \\ g(\dot{\theta}_2) \end{bmatrix} = \begin{bmatrix} u_1 \\ u_2 \end{bmatrix} \quad (6)$$

where θ_1 and θ_2 are the angular position of the flywheels, J_1 and J_2 are the inertia of the flywheels plus that of the motors divided by the square of the gear ratio of the reduction gears, f_1 and f_2 are the effects of the spring, g is the dynamic friction function and finally u_1 and u_2 are the equivalent motor torques applied to the flywheels (see Figure 4). More precisely, the torque contribution given by the spring can be expressed as a function of the two angular positions θ_1 and θ_2:

$$f_1(\theta_1, \theta_2) = M(\theta_1, \theta_2),$$
$$f_2(\theta_1, \theta_2) = -M(\theta_2, \theta_{21}),$$

where

$$M(\alpha, \beta) = \left(-krd + \frac{kl_0rd}{l} \right) \sin\alpha + \left(-r^2k + \frac{r^2kl_0}{l} \right) \sin(\alpha - \beta)$$

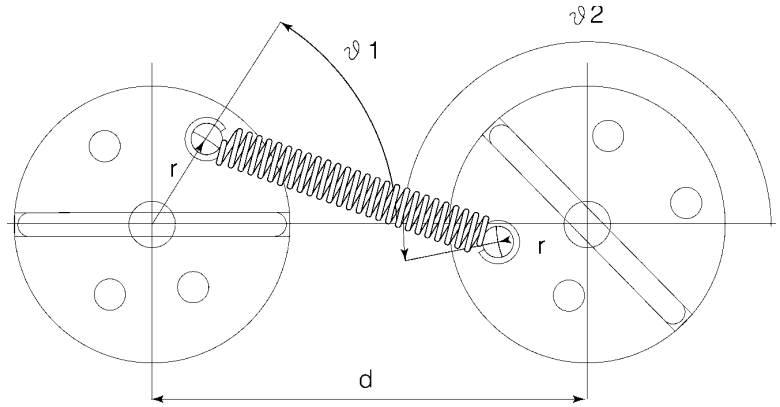

Fig. 4. Plot of the experimental setup.

https://doi.org/10.1017/S0263574799001897 Published online by Cambridge University Press

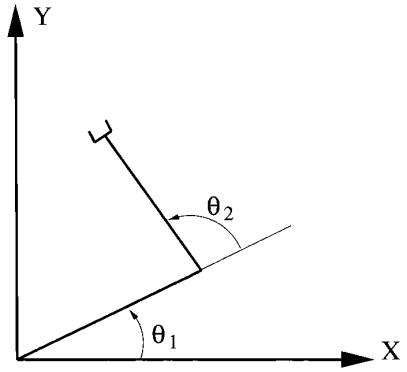

Fig. 5. Kinematic scheme of the SCARA robot.

assuming that r is the distance of the pins from the centre of the flywheels, d is the distance between the centres of the two flywheels, k is the stiffness constant, l_0 is the length of the spring at rest, and finally $l = l(\alpha,\beta)$ is the length of the spring during the motion that is

$$l(\alpha,\beta) = \sqrt{d^2 + 2dr\cos\beta - 2dr\cos\alpha - 2r^2\cos(-\alpha+\beta) + 2r^2}.$$

Some experimental activity has been carried out to identify the parameters of the system. These results permitted the identification of the relative importance of the different effects. In our case the friction and the elastic coupling play a major role. The electronic drives have been configured in such a way that the motors produce a torque proportional to their input set point. The motions of the system have been chosen in order to reproduce actual robot motions; a SCARA robot has been considered (Figure 5), whose links length is 0.33m. It has been ideally assumed that the gripper of the SCARA robot should perform different trajectories (e.g. straight lines or circles) in a chosen time and the corresponding joint rotations have been evaluated by means of the inverse kinematics. These motions have been supplied as set points to the motors of the experimental system. This activity has been repeated for all the analyzed control algorithms to verify their performances.

The controller has been assembled using a standard industrial PC Pentium 166MHz and two industrial I/O cards. One card is used to collect data from the incremental encoders, and to output the torque set point by means of two DAC. The second card has several digital I/O and analog inputs which monitor the motor velocity reading the tachometers and the motor torques reading a test point located in the electronics drivers. The control software has been written in *ANSI C*-language under QNX real-time operating system, which assures a servo loop frequency of 1kHz.

4. RESULTS

All the controllers have been tested on different trajectories in order to prove their effectiveness in different operating conditions. Namely, first of all, a point-to-point motion, with the aim of verifying the steady state errors, has been considered; it consists of a rotation of $\pi/2$ of the flywheels, to be accomplished in 2s, with a "bang-bang" acceleration profile (one second of constant positive acceleration followed by one second of constant negative acceleration).

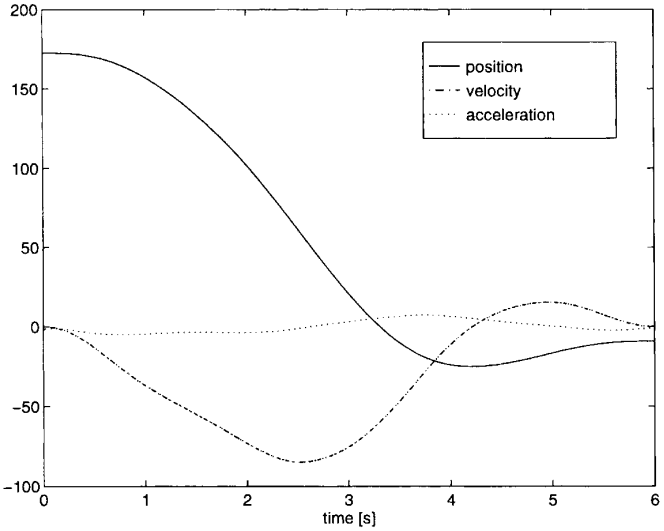

Fig. 6. Position (rad), velocity (rad/s) and acceleration (rad/s^2) setpoints of joint 1 for the linear trajectory.

Then, a linear trajectory from point $(-0.3,0.54)$ to point (0.6,0.15) has been performed in 6s. Finally, a single circular trajectory, centred in (0.33,0.33) and with a diameter of 0.15m, has been executed in 4s. For all these trajectories, the acceleration profile of the end-effector is trapezoidal. In order to better evaluate the executed trajectories, plots of the position, velocity and acceleration reference signals of joint 1 and 2 for the linear trajectory are shown in Figures 6 and 7, respectively, and for the circular trajectory in Figures 8 and 9. It can be noticed how velocities and accelerations are much higher in the latter. Note also that each controller has been tested on the system twice: with and without the spring, in order to evaluate performances in rejecting the disturbance due to the coupling. Discussing the results, the two cases are ferred as "system coupled" and "system not coupled", according to the ISO 9283 standard,[20] the tracking error for the linear and circular trajectories has been calculated as the minimum difference (with sign) between the real end-effector position

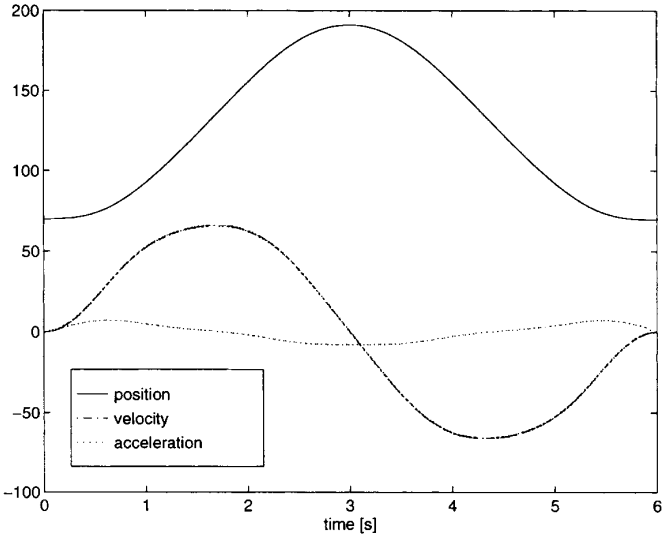

Fig. 7. Position (rad), velocity (rad/s) and acceleration (rad/s^2) setpoints of joint 2 for the linear trajectory.

https://doi.org/10.1017/S0263574799001897 Published online by Cambridge University Press

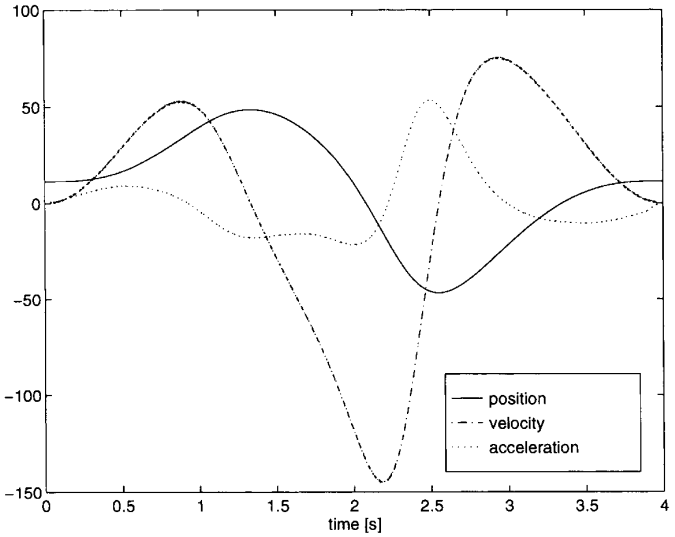

Fig. 8. Position (rad), velocity (rad/s) and acceleration (rad/s^2) setpoints of joint 1 for the circular trajectory.

and the reference trajectory (see Figure 10). To measure the tracking error synthetically, three parameters have been utilized: the maximum absolute error during the trajectory, the RMS error and an error index defined as:

$$\text{e.i.} = \bar{e} + 3\sigma_e$$

where $\bar{e}$ is the average value of the absolute error and σ_e is the standard deviation of the absolute value of e. The definition of e.i. is inspired by the concept of accuracy and repeatability (ISO 9283 standard[20]).

Each controller has been individually tuned as well as possible using the following approaches. The two nested PID controllers has been tuned starting from the Ziegler-Nichols formula and then refining the parameters values using different trajectories in order to obtain, in general, a low tracking error. The velocity loop has been tuned first. Experience showed that the best choice was a PI controller for the velocity loop and a PD controller for the position loop.

The Tarokh's controller has been tuned with similar concept starting from its first term, which is actually a PD, and increasing parameters k and c until an excessive vibration has been noticed. Then, in order to reduce the steady-state error, the second term has been added. In our system, the third term proved to be less significant than the first two, and has been tuned quite easily, substituting the signum function with the saturation function.

Regarding the discontinuous integral control, a tuning procedure can be established, fixing the PD part as well as in the previous case and then increasing h as much as possible, until vibrations occur, in order to keep k as small as possible. Actually, in our system, h is the most significant parameter and k can be very small to avoid chattering. In the discrete version, once the value of c has been fixed, it is necessary to increase k_e in order to decrease the tracking error keeping k small. However, care must be taken not to increase k_e too much, since it is responsible for vibrations too.

In order to verify the accuracy of the tuning phase and the performances of the considered controllers, we performed the same linear motion with different time intervals, from 2s to 6s with a step of 0.5s (note that the motion of 2s requires almost the maximum velocity that can be provided by the motors). Figures 11–14 report the maximum and RMS tracking errors for the end-effector for the motions with different duration, where the different controllers have been adopted for the system both with and without the spring. It can be seen how performances do not decrease significantly when the motion time decreases and therefore the controllers parameters are well-tuned. For the sake of clarity, in the next we refer only to the previously described trajectories in presenting the experimental results. For the

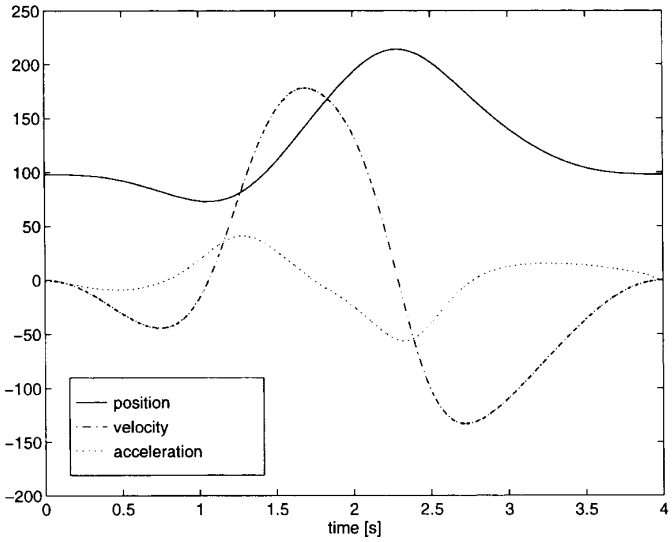

Fig. 9. Position (rad), velocity (rad/s) and acceleration (rad/s^2) setpoints of joint 2 for the circular trajectory.

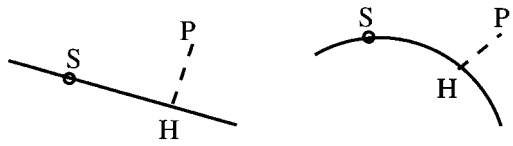

Fig. 10. Tracking error PH for the linear and circular trajectories, where S is the set-point and P is the actual position.

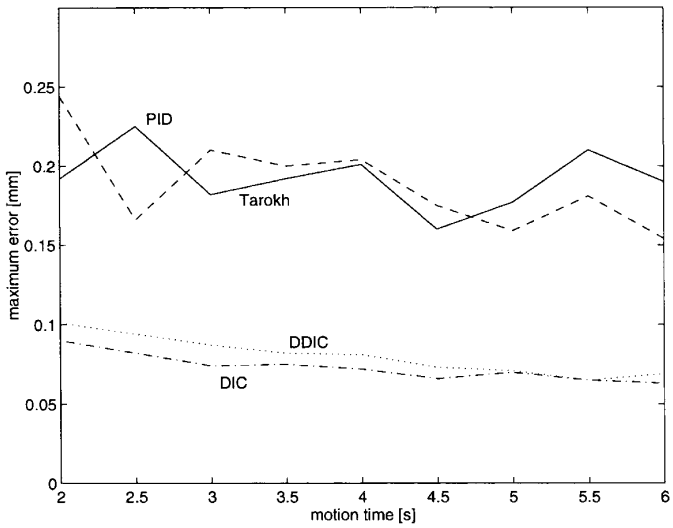

Fig. 11. End-effector maximum tracking errors for the linear motion with different duration, using the controllers for the not coupled system.

https://doi.org/10.1017/S0263574799001897 Published online by Cambridge University Press

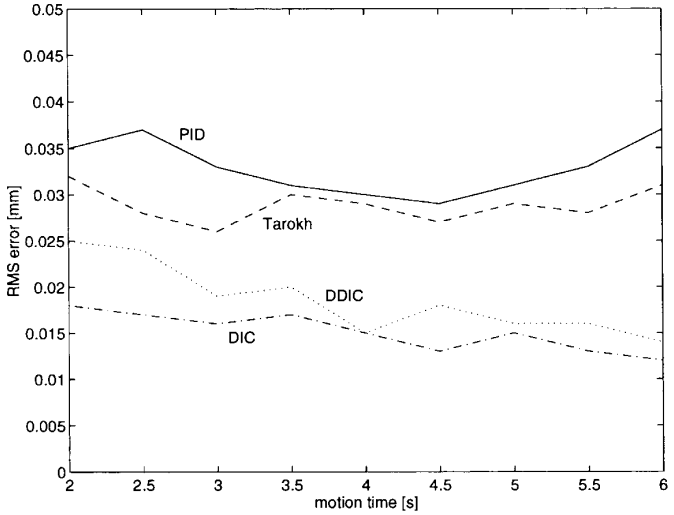

Fig. 12. End-effector RMS tracking errors for the linear motion with different duration, using the controllers for the not coupled system.

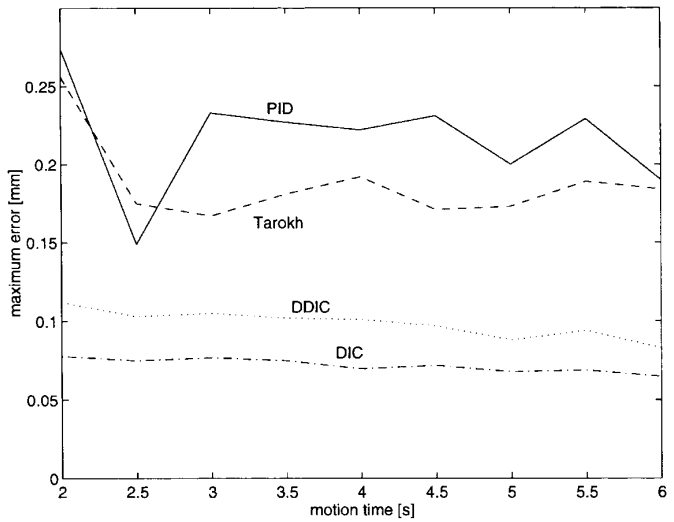

Fig. 13. End-effector maximum tracking errors for the linear motion with different duration, using the controllers for the coupled system.

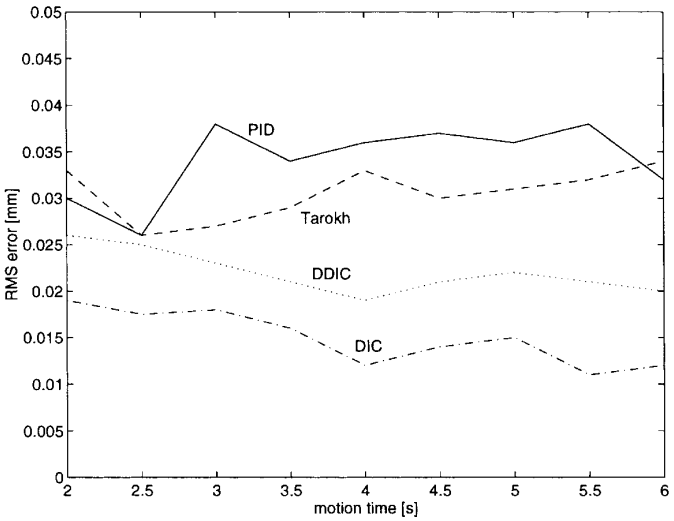

Fig. 14. End-effector RMS tracking errors for the linear motion with different duration, using the controllers for the coupled system.

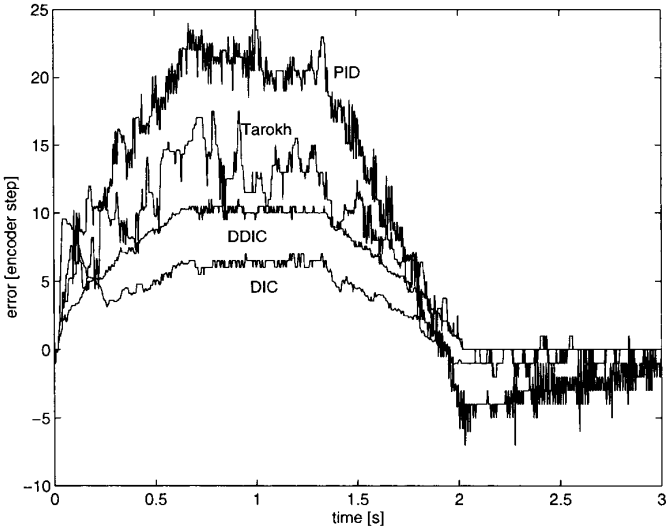

Fig. 15. Tracking errors for point-to-point motion with different controllers. System not coupled.

point-to-point motion all the controllers perform quite well in term of steady state errors, as shown in Figure 15 for the not coupled system. However, it can be noticed how during the motion and also at the end of it, the continuous version of the DIC achieves a lower error and that the PID controller is worse than the others. In fact, the position error is limited to a maximum of 25 encoder steps for the PID and 5 steps for DIC. Furthermore, PID requires more than one second after the end of the motion to reduce the steady-state error under one step. The effect of the coupling spring seems to be well compensated by all the controllers, although Tarokh's regulator appears to perform slightly worse. Plots of the tracking errors for the coupled system are displayed in Figure 16.

The same conclusions can be drawn with respect to the linear and circular trajectories, where the lowest tracking error is achieved by the DIC in its continuous version and the discrete version is better than PID and Tarokh's controllers. Tracking errors of the analyzed controllers versus the PID one are plotted in Figures 17–28, both for the

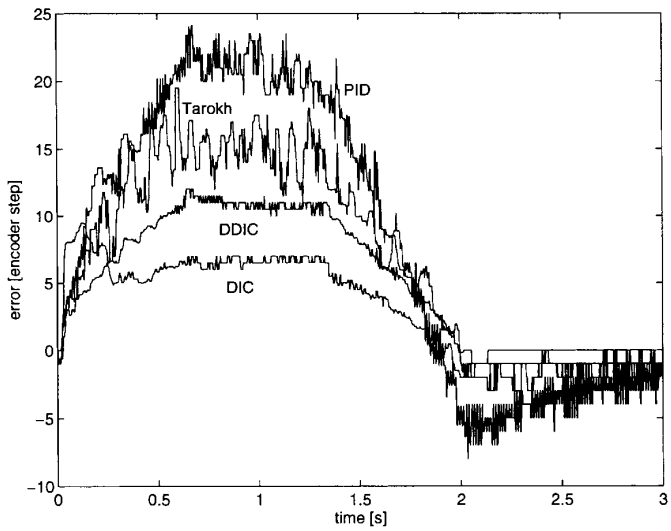

Fig. 16. Tracking errors for point-to-point motion with different controllers. System coupled.

https://doi.org/10.1017/S0263574799001897 Published online by Cambridge University Press

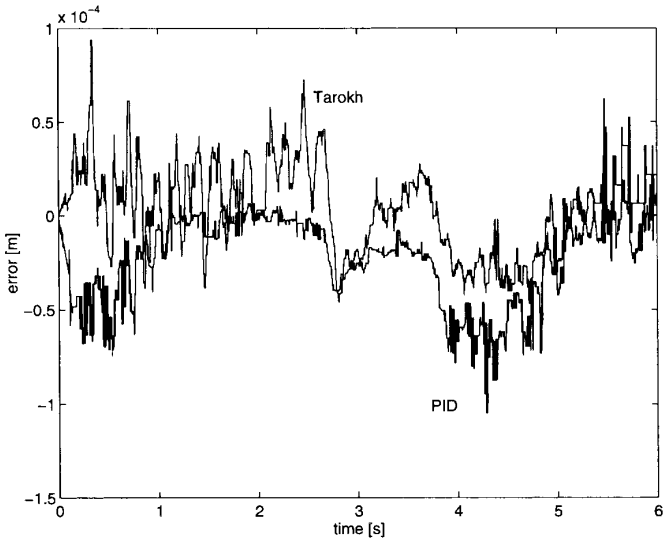

Fig. 17. Tracking errors for the linear trajectory with PID and Tarokh's controllers. System not coupled.

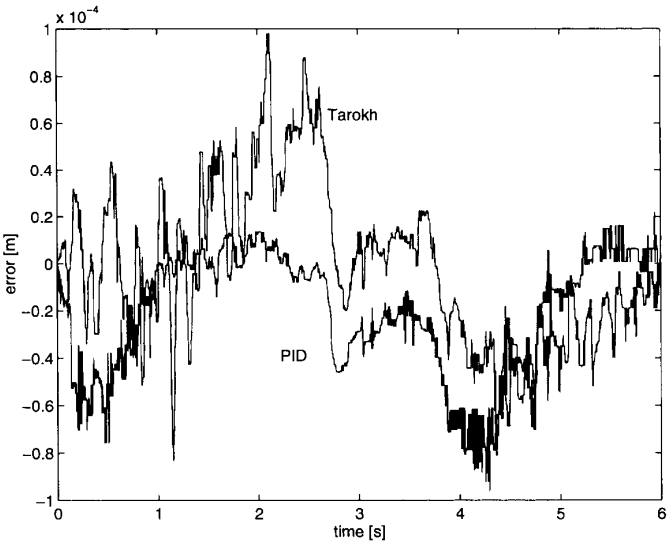

Fig. 18. Tracking errors for the linear trajectory with PID and Tarokh's controllers. System coupled.

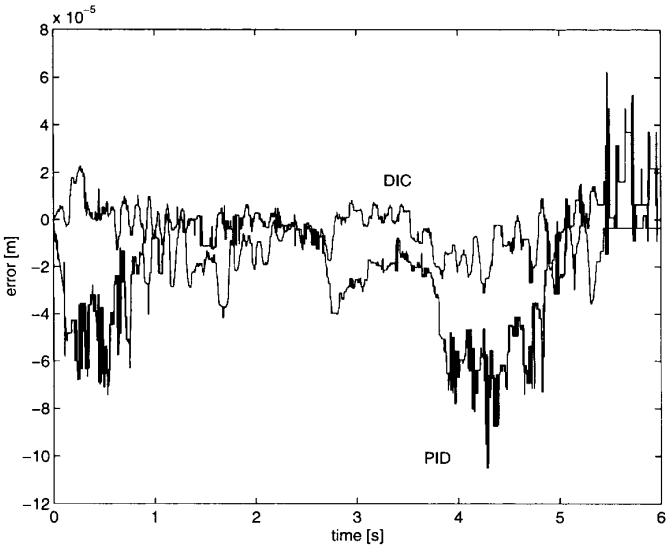

Fig. 19. Tracking errors for the linear trajectory with PID and DIC controllers. System not coupled.

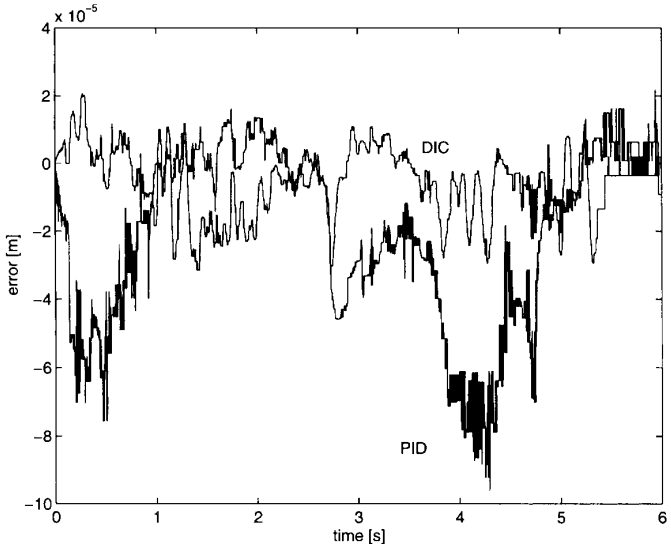

Fig. 20. Tracking errors for the linear trajectory with PID and DIC controllers. System coupled.

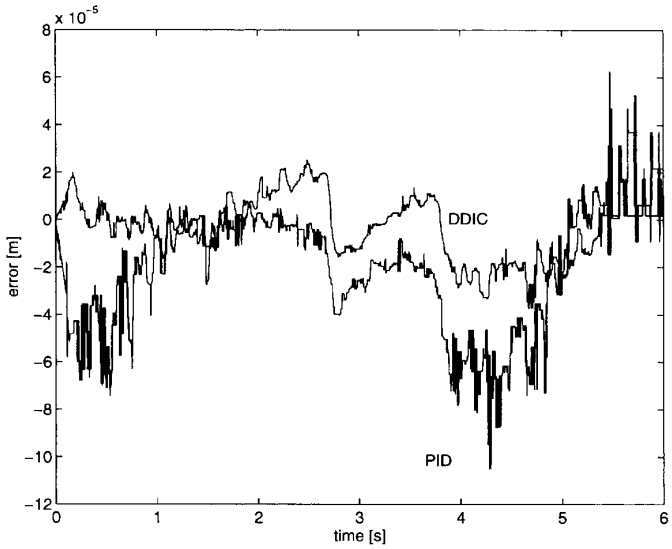

Fig. 21. Tracking errors for the linear trajectory with PID and DDIC controllers. System not coupled.

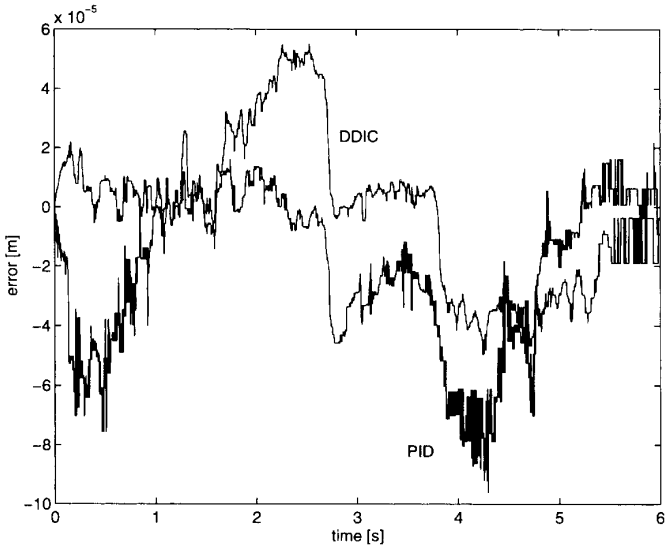

Fig. 22. Tracking errors for the linear trajectory with PID and DDIC controllers. System coupled.

https://doi.org/10.1017/S0263574799001897 Published online by Cambridge University Press

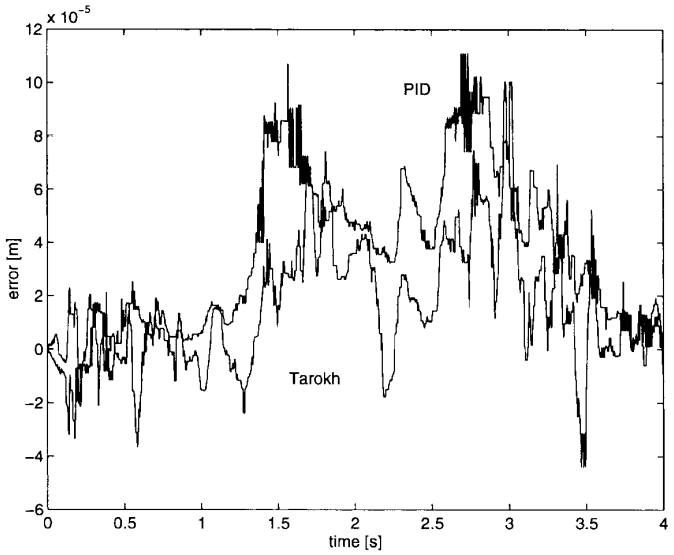

Fig. 23. Tracking errors for the circular trajectory with PID and Tarokh's controllers. System not coupled.

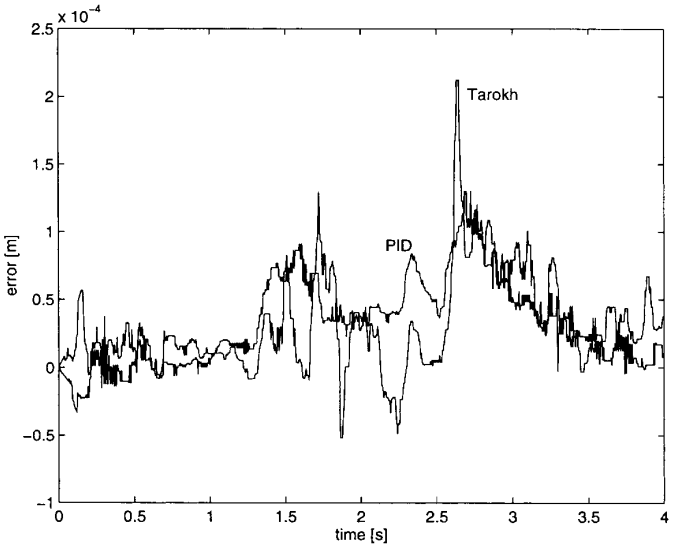

Fig. 24. Tracking errors for the circular trajectory with PID and Tarokh's controllers. System coupled.

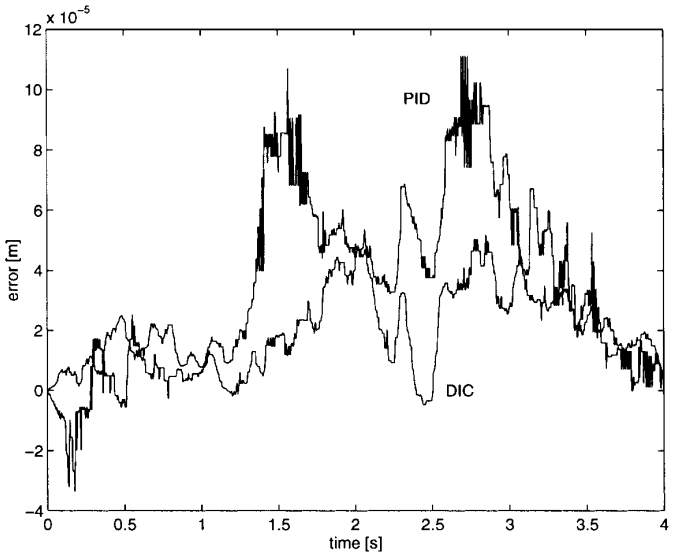

Fig. 25. Tracking errors for the circular trajectory with PID and DIC controllers. System not coupled.

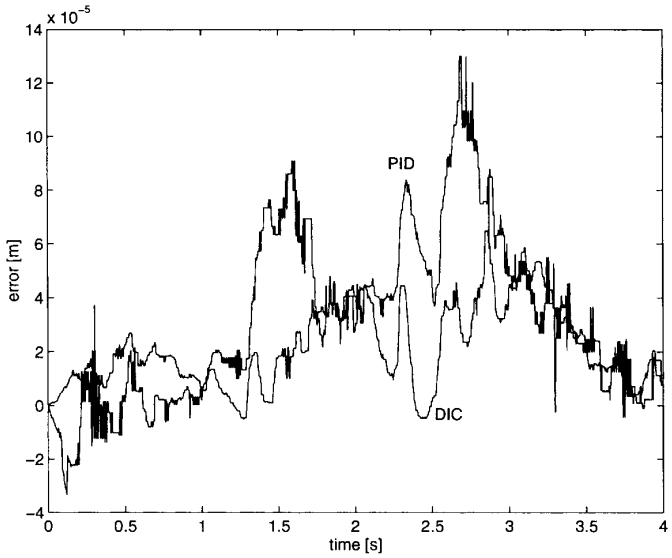

Fig. 26. Tracking errors for the circular trajectory with PID and DIC controllers. System coupled.

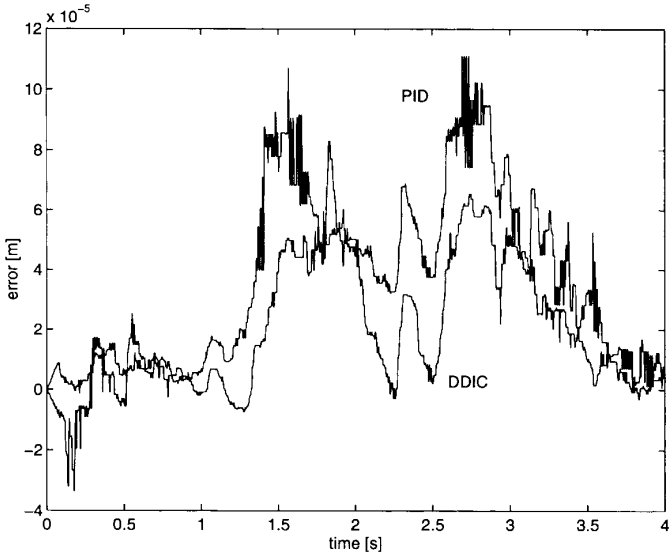

Fig. 27. Tracking errors for the circular trajectory with PID and DDIC controllers. System not coupled.

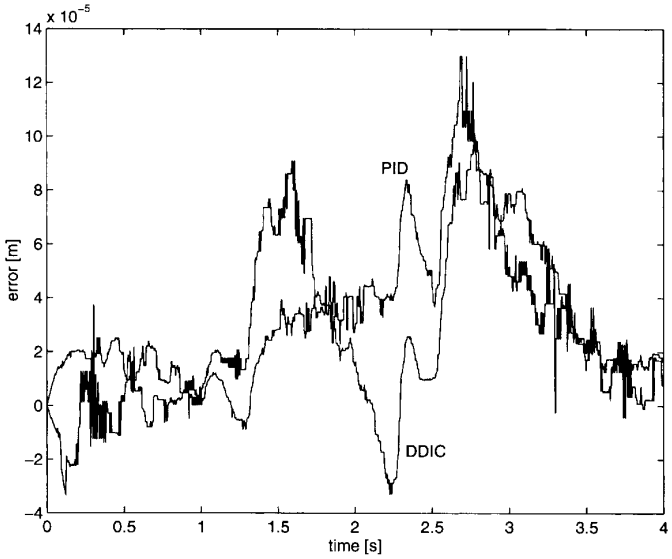

Fig. 28. Tracking errors for the circular trajectory with PID and DDIC controllers. System coupled.

https://doi.org/10.1017/S0263574799001897 Published online by Cambridge University Press

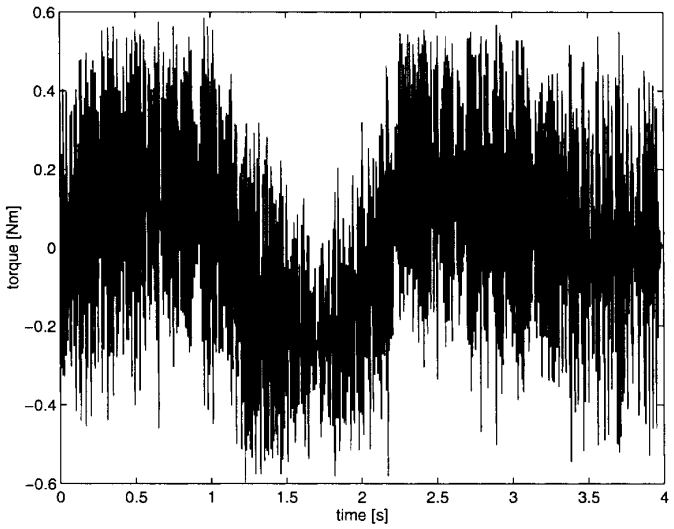

Fig. 29. Torque signal for PID controller.

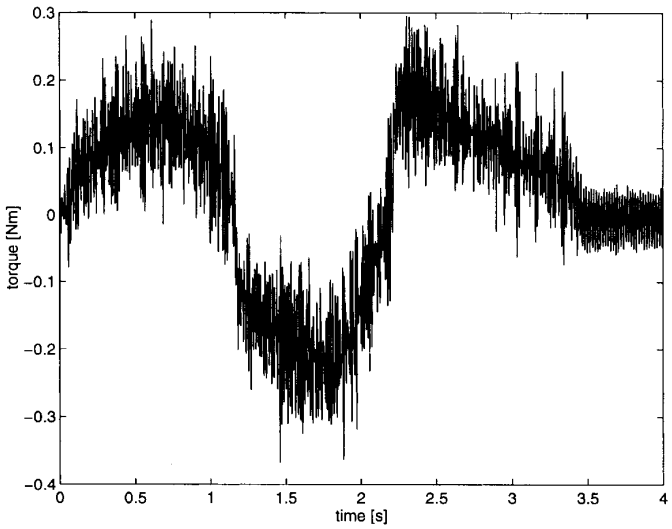

Fig. 31. Torque signal for discontinuous integral controller (DIC).

coupled and non-coupled system. Note that data have been slightly filtered for the sake of clarity. Results are then summarized in Tables I–IV. It is also worth stressing that torque vibrations generated by the two sliding mode controllers are much lower than in the other cases. This is particularly important since it is well known that robot life-span generally decreases when the system has to cope with vibrations, and torque vibrations can excite mechanical vibrations resulting in performance degradation and motor overheading. As an example, the motor torques measured during the circular trajectory, in the case of application of the anlayzed control laws, are plotted in Figures 29–32, referring to the first joint. Note that in all cases the signal has been obtained directly from a test point of the driver and filtered with a low-pass filter at a frequency of 100Hz. The low frequency components represent the torque required to move the flywheels, whilst the high frequency term is the chattering introduced by the controller. In order to measure the chattering amplitude, the torque signals have been filtered off-line using a high pass filter and then the mean of the absolute values has been evaluated, obtaining a "chattering index" c.i. reported in Table V, which underlines against the effectiveness of the two sliding mode controllers.

5. FRICTION COMPENSATION

In order to evaluate the effects of the friction on the tracking capability of the controllers, an identification of the dynamic fraction of both the motors and the gearboxes has been accomplished. This has been done simply by measuring the torques generated after imposing different constant velocities on the two motors and then interpolating the read torques versus velocity by a polynomial function. Measuring the actual motor velocities, it is then possible to predict a value of the torque due to the friction, and add it to the control law. In theory, this should compensate the effects of the friction and improve the trajectory tracking performances. Results are summarized in Tables VI–IX; when compared with Tables I–VI it is evident, however, that the improvement is generally not very significant. This can be

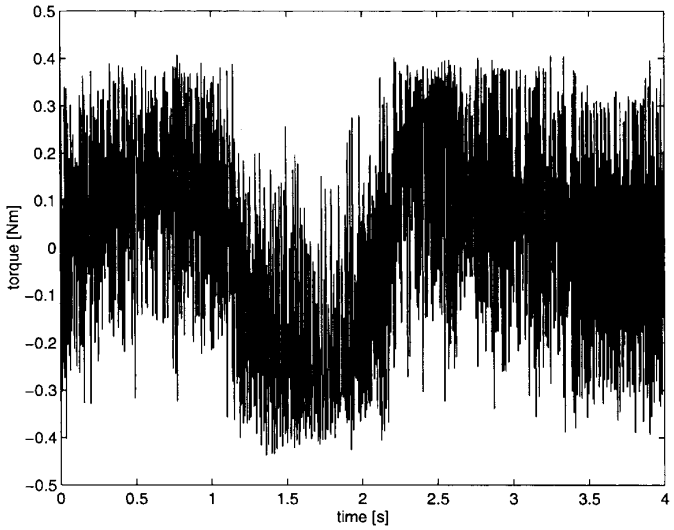

Fig. 30. Torque signal for Tarokh's controller.

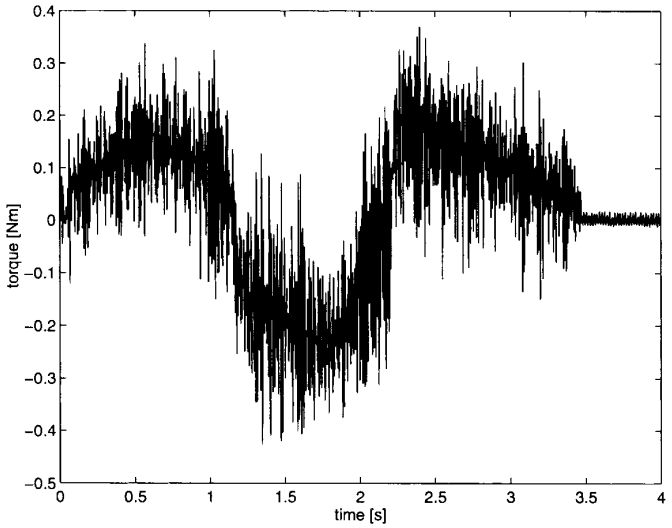

Fig. 32. Torque signal for discontinuous integral controller, discretised version (DDIC).

https://doi.org/10.1017/S0263574799001897 Published online by Cambridge University Press

explained by the fact that the integral terms contained in all the algorithms supply a good prediction of the requested torque. Besides, it must be taken into account that the friction identification procedure is very difficult and time consuming in a real manipulator, because the motors cannot be easily disassembled for testing procedures.

Table I. Tracking error values (in mm) for the linear trajectory. System not coupled.

Controller	max	rms	e.i.
PID	0.194	0.037	0.164
Tarokh	0.154	0.031	0.129
DIC	0.063	0.012	0.050
DDIC	0.069	0.014	0.056

Table II. Tracking error values (in mm) for the linear trajectory. System coupled.

Controller	max	rms	e.i.
PID	0.190	0.032	0.148
Tarokh	0.184	0.034	0.145
DIC	0.065	0.011	0.049
DDIC	0.083	0.020	0.080

Table III. Tracking error values (in mm) for the circular trajectory. System not coupled.

Controller	max	rms	e.i.
PID	0.200	0.045	0.737
Tarokh	0.205	0.036	0.737
DIC	0.088	0.021	0.734
DDIC	0.126	0.021	0.737

Table IV. Tracking error values (in mm) for the circular trajectory. System coupled.

Controller	max	rms	e.i.
PID	0.203	0.052	0.917
Tarokh	0.280	0.045	0.735
DIC	0.092	0.021	0.734
DDIC	0.131	0.034	0.916

Table V. Chattering index of the different controllers for the circular trajectory.

Controller	c.i.
PID	0.215
Tarokh	0.164
DIC	0.043
DDIC	0.063

Table VI. Tracking error values (in mm) for the linear trajectory with friction compensation. System is coupled.

Controller	max	rms	e.i.
PID	0.170	0.030	0.134
Tarokh	0.181	0.029	0.126
DIC	0.064	0.011	0.050
DDIC	0.065	0.011	0.050

Table VII. Tracking error values (in mm) for the linear trajectory with friction compensation. System coupled.

Controller	max	rms	e.i.
PID	0.181	0.035	0.155
Tarokh	0.200	0.035	0.146
DIC	0.065	0.011	0.049
DDIC	0.078	0.017	0.069

Table VIII. Tracking error values (in mm) for the circular trajectory with friction compensation. System not coupled.

Controller	max	rms	e.i.
PID	0.164	0.038	0.737
Tarokh	0.229	0.038	0.737
DIC	0.088	0.018	0.734
DDIC	0.115	0.023	0.737

Table IX. Tracking error values (in mm) for the circular trajectory with friction compensation. System coupled.

Controller	max	rms	e.i.
PID	0.185	0.033	0.916
Tarokh	0.261	0.047	0.735
DIC	0.086	0.020	0.734
DDIC	0.135	0.036	0.916

6. CONCLUSIONS

In this paper we have presented an experimental comparison between different kinds of decentralized controllers for mechanical manipulators. The selected control laws appear to be particularly suitable for use in an industrial context, because of their simplicity and their fault tolerance features. Results show how the conventional PID controller can be effectively substituted by other controllers. In particular, the discontinuous integral control (DIC) appears to be a very good candidate for replacing PID regulators because of the better performances in trajectory tracking, the easy tuning of the parameters and the ability to compensate the dynamic coupling and friction. Moreover, torque vibrations are limited, thereby preventing motor failures.

References

1. J.J. Craig, *Introduction to Robotics: mechanic and control*, Second edition (Addison-Wesley, New York, 1989).
2. J.-J. E. Slotine, W. Li, "On the adaptive control of robot manipulators", *Int. J. Robotics Research*, **6**, 49–59 (1987).
3. D. Gavel and T. Hsia, "Decentralized adaptive control of robot manipulators", *Proc. IEEE Int. Conf. on Robitics and Automation*, Raleigh (1987) pp. 1230–1235.
4. H. Seraji, "Decentralized adaptive control of manipulators: theory, simulation and experimentation", *IEEE Trans. on Robotics and Automation*, **5**, 49–59 (1987).
5. L. Fu, "Robust adaptive decentralized control of robot manipulators", *IEEE Trans. on Automatic Control* **37**, 106–110 (1992).
6. R. Colbaugh, H. Seraji and K. Glass, "Decentralized adaptive control of manipulators", *J. Robotic Systems* **11**, 425–440 (1994).
7. M. Tarokh, Decentralized digital adaptive control of robot motion", *Proc. IEEE Int. Conf. on Robotics and Automation*, Cincinnati, OH (1990) pp. 1410–1415.

https://doi.org/10.1017/S0263574799001897 Published online by Cambridge University Press

8. P. Fraisse and F. Pierrot, “Control of a fast parallel robot: a robust solution”, *Proc. 4th ISRAM* (1992) pp. 319–324.
9. L. Cai and X. Tang, “A model-free decentralized control for robot manipulators”, *Proc. IEEE Int. Conf. on Robitcs and Automation* (1997) pp. 3106–3111.
10. Y. Tang and G. Guerrero, “Decentralized robust control of robot manipulators”, *Proc. American Cont. Conf.* (1998) pp. 992–926.
11. M. Tarokh, “A decentralized nonlinear three-term controller for manipulatory trajectory tracking”, *Proc. IEEE Int. Conf. on Robotics and Automation*, Minneapolis (1996) pp. 3683–3688.
12. A. Nersisian and R. Zanasi, “A modified variable structure control algorithm for stabilization of uncertain dynamical systems”, *Int. J. Robust and Nonlinear Control* **3**, 199–209 (1993).
13. R. Zanasi, “Sliding mode using discontinuous control algorithms of integral type”, *Int. J. Control* **57**, 1079–1099 (1993).
14. C. Bonivento, A. Nersisian, R. Tonielli and R. Zanasi, “A cascade structure for robust control design”, *IEEE Trans. on Aut. Control* **39**, 846–849 (1994).
15. C. Bonivento and R. Zanasi, “Advances in variable structure control”, In: *Colloquim on Automatic Control* (C. Bonivento, G. Marro and R. Zanasi, eds), LNCIS series, Springer Berlin (D) (1996) **Vol. 215**, pp. 177–226.
16. C. Bonivento, M. Sandri and R. Zanasi, “Discrete variable-structure integral controllers”, *Automatica* **34**, 355–361 (1998).
17. K. Åström and T. Hagglund, *PID Controllers: theory, design and tuning* (ISA Press, USA, 1995).
18. F. Esfandiari and H.K. Khalil, “Stability analysis of continuous implementation of variable structure control”, *IEEE Trans. on Automatic Control* **36**, 616–620 (1991).
19. “Special Issue on Sliding Mode Control”, *Int. J. Control* (V.I. Utkin, Guest Ed.) **57**(5), 1003–1259 (May, 1993).
20. ISO 9283:1991, “Manipulating industrial robots: performance criteria and related testing methods”.

https://doi.org/10.1017/S0263574799001897 Published online by Cambridge University Press